Abstract

Plasma microturbulence is a leading candidate of the source of anomalous diffusion observed in tokamak experiments. Global gyrokinetic models have been shown to accurately predict the ion diffusivity, χ_i . Extreme-scale, fixed-flux supercomputing simulations are beginning to simulate modes of operation relevant to next-generation(ITER,DEMO) reactors. Using a surrogate model to reduce the computational expense of XGC simulations, I conduct a predictive scan in ρ^{-1} , to ascertain whether or not the ion diffusivity χ_i scales in a Bohm or gyro-Bohm fashion, and analyze the sensitivity of χ_i to perturbation in the heating model.

Integrated Science Thesis Proposal

Evan Shapiro

Master's of Integrated Science, University of Colorado Denver

February 14, 2018

Contents

1 Introduction **3**

1.1 Fusion as a Source of Energy 3

1.2 Magnetically Confined Fusion 4

1.3 Diffusion, Neoclassical Theory, and Scaling Laws 6

1.4 Gyrokinetic Equations 9

1.5 XGC Code & Heating Models 9

2 Experimental Metholodogy **9**

2.1 Surrogate Models 10

3 Prediction under Uncertainty **11**

3.1 Surrogate Models 12

3.2 Proposed UQ Study 13

3.3 Proposed UQ Study 15

4 Literature Review **16**

Contents

1 Introduction

1.1 Fusion as a Source of Energy

One of the most pressing issues of the 21st century is providing affordable, sustainable, safe energy to the growing world population. As of 2014, there were still 1.1 billion people without access to any form of electricity, with an estimated 3 billion people without access to carbon free energy. Anthropogenically driven climate change has constrained this problem, making policy makers rethink long terms policies regarding coal and natural gas, while safety issues, and public perception, has led to a decreased investment in nuclear fission reactors in the US.

Renewable, clean sources of energy, like large scale solar farms and wind turbine farms, are being adopted in many regions trying to adapt to the energy pressures presented by climate change. In Colorado, Xcel Energy has projected that the solar energy capacity will reach 342 MW by 2019, with 55 percent of all electricity being generated by a mixture of renewable energy sources by 2026. Germany's renewable energy capacity is capable of providing 95 percent of electrical demands at peak output, and expects that renewables will provide 18 percent of all power needs by 2020.

It is tempting to extrapolate on this trend and expect that solar and wind power will eventually replace coal or nuclear fission power plants, however, due to the undependable nature of the sun and the wind, providing continuous electricity requires a base load power supply which has historically been supplied by nuclear fission and coal power plants. Due to the above-mentioned issues, it is desirable to replace the current baseloads with an energy source that is both safe and clean, and magnetic nuclear fusion has the potential to be this replacement energy source.

1.2 Magnetically Confined Fusion

Magnetic nuclear fusion has been studied since the 1960s, but due to the fundamental complexity of controlling a plasma in a fusion reactor sue to issues like, progress in fusion research has stalled. These complexities include understanding the heat transport mechanisms that are unaacounted for by Coulombic interactions in classic transport models, which is the underlying purpose behind this proposal. Due to increasing computational power, as well as international research collaborations, the 21st century has seen a resurgence in interest fusion energy as serious contender for sustainable energy, the most norable being the international thermonuclear experimental reactor (ITER), which will resolve many of the issues that currently stand in the way of a working fusion reactor.

Nuclear fusion is appealing as an energy source due to the net positive energy release that occurs when two light elements collide with enough energy to cause the transfer of a nucleon from one nucleus to the other. In the deuterium-tritium reaction a proton from the deuterium atom is fused to the tritium atom, yielding a release of a neutron, and α particle, and the release of $17.6MeV$ of binding energy. $14.1MeV$ of this binding energy is given to the neutron, and it is this energy that a fusion reactor taps into to power a steam turbine. The nuclear equation for dueterium-tritium reaction is presented below, along with an illustration:

$$D + T \rightarrow \alpha + n + 17.6MeV$$

[1] .

Creating a sustained reaction of a 50-50 % Deuterium-Tritium mixture requires an input of $70KeV$, corresponding to a temperature on the order of $100 * 10^6$K. It is this high temperature environment that leads to the complete ionization of the deuterium-tritium mixture, resulting in a plasma.

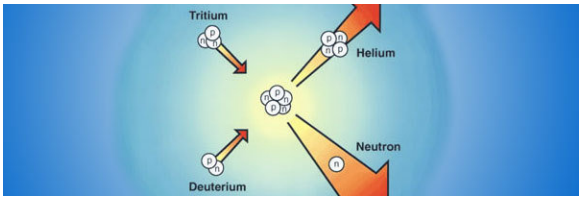

Figure 1: Deuterium-Tritum Reaction Image Courtesy of Max-Planck Institute

More detail will be included below - just need to get ideas down.

Due to the engineering requirements for magnetic pressure, plasma confinement time, and plasma temperature, with the complete explanation of these requirements being beyond the scope of this proposal, a toroidal geometry is the accepted geometry for a fusion reactor. The basic design requirements are as follows. The plasma is contained within the inner cylinder of a toroid, with the first wall of the cylinder being protected by a strong magnetic field that shields the wall from thermal loading from the $14.1MeV$ neutrons, Bremsstrahlung heat loss, and heat conduction. Inside the first wall is the region called the blanket and shield, which is the region of heat exchange for powering an external steam turbine, and provides a tritium breeding ground that sustains the supply of tritium required for the fusion reaction. Outside of this region is the a shield wall which prevents the escape of any radioactive neutrons or gamma particles. The final layer of the toroid contains the superconducting toroidal solenoid, which generates the $10 - 15[T]$ magnetic field inside of the fusion reactor, which again is responsible for confining the ionic and electron components of the plasma inside the reactor. Figures 1 shows the generic theoretical cross-sectional area of toroidal reactor, while figure 2 shows the cross-sectional area of the ARIES-AT tokamak design.

Not shown in the picture is the center, or donut hole, of the toroidal reactor. In current reactors, there is an additional magnet in this region that produces a poloidal magnetic field, which when combined with the toroidal magnetic fields produces the magnetic field lines, as seen in figure 3.

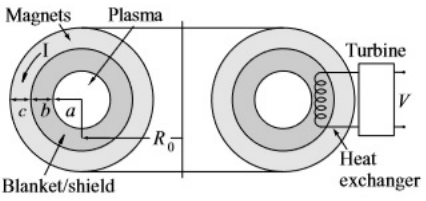

(a) Generic toroidal fusion reactor showing the plasma, blanket-and-shield, and magnets. Image Source J. Friedberg [1]

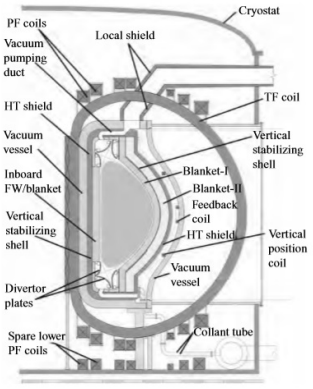

(b) Cross section of the ARIES-AT power core conguration (courtesy of F. Najmabadi). [1]

Due to the Lorentz force, this configuration of magnetic field lines manages to capture the majority of the diffusing ions and electrons in a helical tractory around the magnetic fields lines due to to the Lorentz force on the charged particles.

1.3 Diffusion, Neoclassical Theory, and Scaling Laws

Maintaining a viable, power producing fusion reactor requires that power inputs and outputs be balanced within the reactor. This power balances requires an accounting of all of the power sinks and sources available to the plasma, as well as an accounting of all the transport mechanisms within the plasma. While we are using a 5-D gyrokinetic model in our simulation work, it can be illustrative to use the 0-D conservation of energy equation to demonstrate the basic principle of power balance. The 0-D fluid conservation of energy equation is given by:

$$\frac{3}{2}\frac{\partial p}{\partial t} + \frac{3}{2}\nabla \cdot p\vec{v} + p\nabla \cdot v + \nabla \cdot \vec{q} = S$$

where the internal energy U has been substituted for $\frac{3}{2}p$[1].

Let's analyze this equation: The first term accounts for the variation of energy flowing into and out of the system with respect to time, the second term accounts for energy lost or gained due to convection of heat out of the system, the third term accounts for energy losses due to compression

and expansion of the plasma within a reactor, the 4th term account for heat losses due to diffusion and conduction, and S accounts for the sources and sinks available to the plasma. The sources are the α particle heating due to the D-T nuclear reaction and any auxiiliary heating being supplied to the plasma, while the sinks are the neutrons escaping the plasma into the blanket surrounding the reactor, and Bremsstrahlung radiation.

Assuming that the power production in the reactor has reached a steady state the time term drops out, as well as the convection and compression terms, leaving the 0-D energy conservation equation:

$$\nabla \cdot \vec{q} = S.$$

This equation makes intuitive sense. In equillibrium, if the diffusive processes are matched by the power sources sources and sinks, then a power balance will be achieved in the equation. If the diffusion of heat out of the system increases, α particle heating has to increase to maintain power balance in the reactor, decreasing the efficiency of the reactor.

Maintaining a plasma reactor with a viable power output requires that the transport of heat out of the plasma be balanced by the alpha heating power of the plasma. Characterizing the heat conduction parameter, or ion heat diffusivity χ_i, in a plasma is current research, [2] [3] as it is the primary heat loss mechanism in a tokamak reactor. Per Friedberg In a plasma there are three important types of transport: heat conduction, particle diffusion, and magnetic eld diffusion. Of these, heat conduction is the most serious loss mechanism... [1]."

Classic and neoclassical diffusion model the ion heat diffusivity using a random walk model of the ions and electrons as they move through their gyrokinetic trajectory around the magnetic field lines in the toroidal reactor, interacting with other charged species along their trajectory, and imparting thermal energy. Neoclassical transport theory refers to the diffusion process within a toroidal geometry, which generates for a 2.4 fold increase in ion heat diffusion.

The classical and neoclassical models are unable to account for the observed, anomalously large transport of energy and particles across the confining magnetic field. It is assumed that that the anomolous ionic thermal diffusivity is a function of various local dimensionless quantities, including β the ratio of plasma to magnetic pressure, ρ^*, which is explained below. Current research [2] focuses on plasma microturbulence caused by steep ionic thermal gradients as the driving mechanism for this anomalous heat transport, and incorporates scaling arguments in ρ^* to make predictions using available data from smaller scale fusion reactors to predict how ion heat diffusivity will scale to ITER levels. Scaling laws are laws used in fluid dynamics that are allowed to be made under dynamic and geomtric similarity situations, thus since the dynamics and geometries between tokamaks is nearly identical, scaling laws are useful when experimental validation is not available.

We define ρ^* to be $\rho^* = \rho_i/a$ where ρ_i is the gyrokinetic radius of the ion as it moves around the magnetic field in its trajectors through the fusion reactor, and a is the minor radius of the tokamak, or the radius of the inner cross-sectional area of the tokamak. The reason that ρ^* is interesting is because "Existing experimental devices can match all of these transport relevant dimensionless parameters expected in a reactor scale with the exception of ρ^* [4]." The inability to set the parameter rho^* in a lab experiment, and the advanced modeling and simulation capabilities of current tech, make a new study on ionic thermal diffusivity an ideal topic for a master's thesis

Thus, the stated purpose of this thesis is to determine how the ionic thermal diffusivity scales with a scan in ρ^* up to ITER scales, to determine whether the diffusion becomes Bohm or gyro-Bohm like. Bohm diffusion indicates that the diffusin increases linearly with temperature, and is undesireable, while gyro-Bohm diffusion indicates that the diffusion scales sublinearly with temperature, and is desireable.

We will use available fusion reactor data, and implement surrogate modeling techniques to reduce the computational expense of running a simulation of t5-D full-fidelity gyrokinetic model. The out-

come of this project will be a pdf of the ion diffusion, with uncertainties. Once this is accomplished, if time permits, we will perform a push forward sensitivity analysis, by perturbing χ_i within the the full 5-D heating model.

1.4 Gyrokinetic Equations

1.5 XGC Code & Heating Models

2 Experimental Metholodogy

Prediction under uncertainty is often an expensive and complicated process[5, 6]. The tradeoff between the computational cost of complex models and the loss of predictive accuracy associated with simpler models may be addressed by emerging multifidelity UQ approaches[7, 8].

In magnetic confinement fusion, there is an important, clearly defined set of prediction scenarios, corresponding to modelling future reactor(ITER/DEMO) performance. Even a "high-fidelity", extreme-scale model such as XGC, still has a parameter space of large enough dimension to make a brute-force, sampling-based predictive process impossible. The traditional approach to prediction, with or without extrapolation, is to sample the model parameter input space $\theta = \theta_1, \theta_2, \ldots, \theta_d$, evaluate the model, and return a quantity of interest (QoI) $Q(\theta)$. Most realistic QoI maps are nonlinear in the QoI map(even if the governing PDE is linear), so the probability distribution function(PDF) of $Q(\theta)$ will have to be estimate in a non-parametric way, typically by kernel density estimation, or by computing empirical statistics from samples. The mean-integrated squared error of the approximate PDF converges with a rate of $\mathcal{O}(N^{-2/(d+4)})$, where N is the number of samples of the model and d is the dimension of the input space. As each sample typically involves a PDE solve and subsequent post-processing, this process quickly becomes exorbitantly expensive.

2.1 Surrogate Models

A surrogate model replaces the large cost of the model solve with a fast, explicit function evaluation. The surrogate model is constructed via interpolation or regression on a modest number of potentially deterministic traning samples M. The error from insufficient samples in the kernel density estimation is exchanged for the error between the true QoI $Q(\theta)$ and surrogate QoI $Q_S(\theta)$[9]. Sparse grid approaches [10, 11] give roughly the same error(modulo a factor of n^{d-1}, where d is the dimension of the (input) parameter space and n is the number of training points)) as traditional tensor-product surrogates. However, the number of samples is $\mathcal{O}(2^n n^{d-1})$, instead of the full grid cost of $\mathcal{O}(2^{nd})$. These savings and accuracy can potentailly be increased by adopting adaptive sparse grid surrogates[10].

Augmented Surrogates

In predictive extrapolation, the target scenario for $Q(\theta)$ is often sufficiently expensive to even make the surrogate approach tenuous. One strategy in this situation is to construct the surrogate using a sequence of lower-fidelity models to construct $\tilde{Q}(\theta)$, and then train the surrogate[8]. This often requires a good characterization of the error between $Q(\theta)$ and $\tilde{Q}(\theta)$. This is not a well-explored or understood area in the kinetic plasma PIC community.

Another approach is to add deterministic parameters that describes "nearby" scenarios, s.t. $Q(\theta) = A(\theta, k_1, k_2, \ldots, k_r)$, k_i fixed. We call the determanistic parameters k_i augmentation parameters, and the surrogate model A_S of A, the augmented surrogate. Moderate gains are achieved when the number of augmentation parameters is small and the cost of sampling A outside of the prediction scenario Q is much cheaper. If the gradient of A with respect to θ is only weakly dependent on the augmentation parameters, significant (cost-based) accuracy savings can be achieved.

¡¡¡¡¡¡¡ HEAD There are two fundmental assumptions in the construction of an augmented surrogate of a n-dimensional predictive scenario $Q(\theta_1, \theta_2, \ldots, \theta_n)$.

1. There exists small number m of (usually deterministic) parameters $d_1, d_2, \ldots, d_m$ that characterize nearby n-dimensional predictive scenarios $\tilde{Q}_i(\theta_1, \theta_2, \ldots, \theta_n)$.

2. The cost of a sample from the nearby scenario, $C_{\tilde{Q}_i}$, is much less than the cost C_Q of a sample from the desired prediction scenario.

=======

3 Prediction under Uncertainty

Prediction under uncertainty is often an expensive and complicated process[5, 6]. The tradeoff between the computational cost of complex models and the loss of predictive accuracy associated with simpler models may be addressed by emerging multifidelity UQ approaches[7, 8].

In magnetic confinement fusion, there is an important, clearly defined set of prediction scenarios, corresponding to modelling future reactor(ITER/DEMO) performance. Even a "high-fidelity", extreme-scale model such as XGC, still has a parameter space of large enough dimension to make a brute-force, sampling-based predictive process impossible. The traditional approach to prediction, with or without extrapolation, is to sample the model parameter input space $\theta = \theta_1, \theta_2, \ldots, \theta_d$, evaluate the model, and return a quantity of interest (QoI) $Q(\theta)$. Most realistic QoI maps are nonlinear in the QoI map(even if the governing PDE is linear), so the probability distribution function(PDF) of $Q(\theta)$ will have to be estimate in a non-parametric way, typically by kernel density estimation, or by computing empirical statistics from samples. The mean-integrated squared error of the approximate PDF converges with a rate of $\mathcal{O}(N^{-2/(d+4)})$, where N is the number of samples of the model and d is the dimension of the input space. As each sample typically involves a PDE solve and subsequent post-processing, this process quickly becomes exorbitantly expensive.

3.1 Surrogate Models

A surrogate model replaces the large cost of the model solve with a fast, explicit function evaluation. The surrogate model is constructed via interpolation or regression on a modest number of potentially deterministic traning samples M. The error from insufficient samples in the kernel density estimation is exchanged for the error between the true QoI $Q(\theta)$ and surrogate QoI $Q_S(\theta)$[9]. Sparse grid approaches [10, 11] give roughly the same error(modulo a factor of n^{d-1}, where d is the dimension of the (input) parameter space and n is the number of training points)) as traditional tensor-product surrogates. However, the number of samples is $\mathcal{O}(2^n n^{d-1})$, instead of the full grid cost of $\mathcal{O}(2^{nd})$. These savings and accuracy can potentailly be increased by adopting adaptive sparse grid surrogates[10].

Augmented Surrogates

In predictive extrapolation, the target scenario for $Q(\theta)$ is often sufficiently expensive to even make the surrogate approach tenuous. One strategy in this situation is to construct the surrogate using a sequence of lower-fidelity models to construct $\tilde{Q}(\theta)$, and then train the surrogate[8]. This often requires a good characterization of the error between $Q(\theta)$ and $\tilde{Q}(\theta)$. This is not a well-explored or understood area in the kinetic plasma PIC community.

Another approach is to add deterministic parameters that describes "nearby" scenarios, s.t. $Q(\theta) = A(\theta, k_1, k_2, \ldots, k_r)$, k_i fixed. We call the determanistic parameters k_i augmentation parameters, and the surrogate model A_S of A, the augmented surrogate. Moderate gains are achieved when the number of augmentation parameters is small and the cost of sampling A outside of the prediction scenario Q is much cheaper. If the gradient of A with respect to θ is only weakly dependent on the augmentation parameters, significant (cost-based) accuracy savings can be achieved.

There are two fundmental assumptions in the construction of an augmented surrogate of a n-dimensional predictive scenario $Q(\theta_1, \theta_2, \ldots, \theta_n)$.

1. There exists small number m of (usually deterministic) parameters $d_1, d_2, \ldots, d_m$ that characterize nearby n-dimensional predictive scenarios $\tilde{Q}_i(\theta_1, \theta_2, \ldots, \theta_n)$.

2. The cost of a sample from the nearby scenario, $C_{\tilde{Q}_i}$, is much less than the cost C_Q of a sample from the desired prediction scenario.

The *augmented surrogate* is a surrogate model $A(\theta, d)$ constructed on training data $\{(\theta, d), \hat{Q}(\theta, d)\}$ in the $m + n$-dimensional parameter space.

Adaptive sparse grid method

The classical sparse grid method is dimension agnostic[10]. All interactions of the same order are treated equally. Often, a small subset of variables and interactions contributes significantly to the variability of the function $Q(\theta, d)$. If the variability in the θ-dimensions is greater than the variability in the scenario parameters($\{d_i\}$) then the overall cost of constructing the larger dimensional surrogate is actually less, due to the cheaper computational cost of $\tilde{Q}_i$.

We modify the greedy algorithm for constructing h-adaptive generalized sparse grid (h-GSG) in [11]. The hierarchical surpluses for the current sparse grid are modified with a cost weight $W_C(d_1, d_2, \ldots, d_m)$ that approximates the relative cost of simulating the added sparse grid point, and a m-dimensional distance metric that penalizes sparse grid samples that are too far away from the prediction scenario $Q(\theta)$. This encourages parameter exploration in θ_i-dimensions at inexpensive simulation levels, while rewarding coarse grid points that reduce the local surrogate error near the prediction scenario $Q(\theta)$.

3.2 Proposed UQ Study

We will conduct a base parameter scan in (ρ_*), at the mean values of the uncertain inputs. This will verify that wedge, Eulerian versus PIC, or other factors do not impact the conclusions reached in [2]. This scan will also provide the first training runs for the augmented surrogate A.

Data from a range of ρ_*^{-1} simulations will be obtained in the interval (100,600) will be provided by Varis Carey and other members of the BPS Scidac team from simulations run at NERSC and Oak Ridge facilites. A budget of 20,000 SU at NERSC has been allocated for providing the data for this scaling study(which is already partially complete at the time of this proposal) and for additional simulations to train the augmented surrogate to cover the input parameter space. The main input parameters parameterize the location, slope, and shape of the core heat source and boundary sink. Additional parameters covering torque will be allowed if the computational budget allows further investigation. If NERSC resources are expended, certain (small-scale) simulations will be conducted on CU-Denver or RMCC resources(Summit) under the supervision of Varis Carey.

Postprocessing Software

Postprocessing software (python and Matlab) are available to extract plasma QoI from XGC 2D and 1D diagnostic output. The BPS team will arrange a NERSC account to avoid transfer of large binary files and allow simulation data to be repurposed for future studies.

Evan: you won't be expected to do any major software development(mainly just modify some scripts, maybe improve them) as part of this project.

The *augmented surrogate* is a surrogate model $A(\theta, d)$ constructed on training data $\{(\theta, d), \hat{Q}(\theta, d)\}$ in the $m + n$-dimensional parameter space.

Adaptive sparse grid method

The classical sparse grid method is dimension agnostic [12]. All interactions of the same order are treated equally. Often, a small subset of variables and interactions contributes significantly to the variability of the function $Q(\theta, d)$. If the variability in the θ-dimensions is greater than the variability in the scenario parameters($\{d_i\}$) then the overall cost of constructing the larger dimensional surrogate is actually less, due to the cheaper computational cost of $\tilde{Q}_i$.

We modify the greedy algorithm for constructing h-adaptive generalized sparse grid (h-GSG)

in [11]. The hierarchical surpluses for the current sparse grid are modified with a cost weight $W_C(d_1, d_2, \ldots, d_m)$ that approximates the relative cost of simulating the added sparse grid point, and a m-dimensional distance metric that penalizes sparse grid samples that are too far away from the prediction scenario $Q(\theta)$. This encourages parameter exploration in θ_i-dimensions at inexpensive simulation levels, while rewarding coarse grid points that reduce the local surrogate error near the prediction scenario $Q(\theta)$.

3.3 Proposed UQ Study

We will conduct a base parameter scan in (ρ_*), at the mean values of the uncertain inputs. This will verify that wedge, Eulerian versus PIC, or other factors do not impact the conclusions reached in [2]. This scan will also provide the first training runs for the augmented surrogate A.

Data from a range of ρ_*^{-1} simulations will be obtained in the interval (100,600) will be provided by Varis Carey and other members of the BPS Scidac team from simulations run at NERSC and Oak Ridge facilites. A budget of 20,000 SU at NERSC has been allocated for providing the data for this scaling study(which is already partially complete at the time of this proposal) and for additional simulations to train the augmented surrogate to cover the input parameter space. The main input parameters parameterize the location, slope, and shape of the core heat source and boundary sink. Additional parameters covering torque will be allowed if the computational budget allows further investigation. If NERSC resources are expended, certain (small-scale) simulations will be conducted on CU-Denver or RMCC resources(Summit) under the supervision of Varis Carey.

Postprocessing Software

Postprocessing software (python and Matlab) are available to extract plasma QoI from XGC 2D and 1D diagnostic output. The BPS team will arrange a NERSC account to avoid transfer of large binary files and allow simulation data to be repurposed for future studies.

4 Literature Review

Literature Review for MIS Thesis Proposal Ralph C. Smith - Uncertainty Quantification

Determining the plasma size scaling of the ion diffusivity, and performing efficient sensitivity analysis on the ion diffusivity in the heating component of the XCG model, within a constructed surrogate model, will require a knowledge base in the following subjects.

Physics

A background in plasma physics, and the component of the XCG model that is used to model plasma heating and ion diffusivity. To support my physical understanding while completing this research I have identified the following references.

Plasma Physics and Fusion Reactors

Jeffrey P. Friedberg Plasma Physics and Fusion Energy

This textbook covers the physics of plasma fusion, its applications as an energy sources, the physical requirements to create an energy producing fusion reactor, and the designs requirements for fusion reactor with a toroidal geometry - the geometry of the ITER fusion reactor.

XCG Modeling

Dr. Wei-Lee from the Princeton Plasma Fusion Physics Laboratory has posted the lecture notes and homework assignments from a course on Theory and Modeling of Kinetic Plasmas on his website.

http://w3.pppl.gov/ wwlee/

This course contains the background information on gyrokinetic model that is being used to describe the plasma boundary physics in the ITER Tokamak reactor.

Project Description

The project proposal from the Partnership Center for High-Fidelity Boundary Plasma Simulation provides the motivation for performing this research, as well as a reference list containing relevant literature that will be reviewed and cited as necessary.

Case Study to Understand Current Methods in Uncertainty Quantification

I am currently reviewing a paper referenced from the project proposal titled Improved profile fitting and quantification of uncertainty in experimental measurements of impurity transport coefficients using Gaussian process regression by Chilenski et al. to develop an understanding of the uncertainty quantification and parameter estimation pipeline.

Uncertainty Quantification

Performing the sensitivity analysis, and constructing surrogate models will require background knowledge in statistics, both Bayesian and frequ error analysis, uncertainty quantification, and surrogate models. Two textbooks have been identified to support this work.

Uncertainty Quantification: Theory, Implementation, and Applications by Ralph C. Smith

Data Reduction and Error Analysis for the Physical Sciences by Phillip R. Bevington and D. Keith Robinson

References

[1] Jeffrey P. Friedberg, *Plasma Physics and Fusion Energy.* New York: Cambridge University Press, 1st ed., 2007.

[2] Yasuhiro Idomura and Motoki Nakata, "Plasma size and power scaling of ion temperature gradient driven turbulence," *AIP Physics of Plasmas*, vol. 21, p. 5, Feb. 2018.

[3] Choong-Seock Chang et al, "Partnership Center for High-Fidelity Boundary Plasma Simulation Project Proposal," 2017.

[4] G. M. et al, "Non-dimensional scaling of turbulence characteristics and turbulence diffusivity," *Nuclear Fusion*, vol. 41, no. 9, 2001.

[5] J. T. Oden, R. Moser, and O. Ghattas, "Computer predictions with quantified uncertainty, Part I," *SIAM News*, vol. 43, November 2010.

[6] J. T. Oden, R. Moser, and O. Ghattas, "Computer predictions with quantified uncertainty, Part II," *SIAM News*, vol. 43, December 2010.

[7] L. Ng and M. Eldred, "Multifidelity uncertainty quantification using nonintrusive polynomial chaos and stochastic collocation," in *Proceedings of the 53rd AIAA/ASME/ASCE/AHS/ASC Structures, Structural Dynamics and Materials Conference (14th AIAA Non-Deterministic Approaches Conference)*, 2012.

[8] B. Peherstorfer, K. Willcox, and M. Gunzburger, "Survey of multifidelity methods in uncertainty propagation, inference, and optimization," *Technical Report, Aerospace Computational Design Laboratory*, no. TR-16-1, 2016.

[9] T. Butler, C. Dawson, and T. Wildey, "Propagation of uncertainties using improved surrogate models," *SIAM/ASA Journal on Uncertainty Quantification*, vol. 1, no. 1, pp. 164–191, 2013.

[10] H.-J. Bungartz and M. Griebel, "Sparse grids," *Acta Numerica*, vol. 13, p. 147269, 2004.

[11] J. D. Jakeman and S. G. Roberts, "Local and dimension adaptive sparse grid interpolation and quadrature," *CoRR*, vol. abs/1110.0010, 2011.

[12] H.-J. Bungartz, *Sparse Grids*. Cambridge University Press, 2004.